

Microbial symbionts buffer hosts from the consequences of environmental stochasticity

Joshua C. Fowler^{a,b,1}, Shaun M. Ziegler^c, Kenneth D. Whitney^c, Jennifer A. Rudgers^c, and Tom E.X. Miller^a

This manuscript was compiled on July 27, 2023

limit = 188 out of 250 words Species' persistence in increasingly variable future climates will depend on endurance of the detrimental effects of environmental stochasticity. Most organisms host microbiota that shield against stressful environmental conditions, but pinpointing microbial symbioses as buffers against the fitness costs of stochasticity requires experiments covering long-term variability. Here, we use stochastic demographic models for seven plant species parameterized with a 14-year symbiont-removal experiment to demonstrate that microbial symbionts elevate host fitness by dampening year-to-year fluctuations in demographic performance. We show that *Epichloë* fungal endophytes reduce variance in the fitness of their grass hosts by greater than 10% on average across species and that reductions of up to 50% occur for some hosts. Hosts with "fast" life histories that lack longevity as an intrinsic buffer experienced the greatest benefits. Contributions to fitness from variance buffering were modest compared to symbiont benefits to mean fitness under the contemporary climate regime. Simulations of increased environmental stochasticity amplified the value of variance buffering, which surpassed symbionts' mean effects that have dominated most prior research. These results establish microbial-mediated variance buffering as an important yet cryptic mechanism of resilience to increasing stochasticity under global change.

stochasticity | microbial symbiosis | demography | mutualism

Global climate change involves increases in environmental variability, including changes to precipitation patterns and the frequency of extreme weather events (1, 2). Yet, the ecological consequences of increased variability are less well understood than those of changing climate means, such as long-term warming or drying. Incorporating environmental variability into forecasts of population dynamics can improve predictions of the future. Classic theory predicts that long-term population growth rates (equivalently, population mean fitness) will decline under increased environmental variability because the costs of bad years outweigh the benefits of good years – a consequence of nonlinear averaging (3, 4). For example, in unstructured populations, the long-term stochastic growth rate in a fluctuating environment (λ_s) will always be lower than the average growth rate ($\bar{\lambda}$) by an amount proportional to the environmental variance (σ^2):

$$\log(\lambda_s) \approx \log(\bar{\lambda}) - \frac{\sigma^2}{2\bar{\lambda}} \quad [1]$$

Populations structured by size or stage similarly experience costs of variability (5, 6). There are accordingly two pathways to increase population viability in a variable environment: increase the mean growth rate and/or dampen temporal fluctuation in growth rates, also called "variance buffering".

Both the characteristics of species and the properties of their environment can buffer demographic fluctuations, including life history traits such as longevity (7, 8), correlations among vital rates (9), transient shifts in population structure (10), the magnitude of environmental variability (11), or the degree of environmental autocorrelation (12, 13). These factors determine the risks of extinction faced by populations (14) and underlie management strategies promoting ecosystem resilience (15). Yet little is known about how biotic interactions influence demographic variability or contribute to variance buffering (16).

Most multicellular organisms host symbiotic microbes that affect growth and performance (17, 18), and many of these are transmitted via reproduction from maternal hosts to offspring (19). This process of vertical transmission links the fitness of hosts and symbionts in a feedback loop that selects for mutual benefits (20). Many vertically-transmitted microbes are mutualistic and protect hosts from stressful environmental conditions including drought, extreme temperatures, or natural

Significance Statement

limit = 120 out of 120 words
Many symbiotic microbes benefit hosts under environmental stress, which is become more frequent in an increasingly variable climate. Using long-term field experiments with a plant-fungal endophyte model system, we show that, by limiting host exposure to environmental extremes, microbial symbionts reduce their hosts' demographic variance. Because such variance has negative fitness consequences, our results identify variance buffering a novel pathway of host-symbiont mutualism. Species with faster life histories were more strongly buffered by symbiosis, suggesting that microbial symbionts can compensate for the lack of intrinsic tolerance of variability conferred by "slow" life history traits. Simulations revealed that increasing stochasticity intensifies the benefits of variance buffering, suggesting a key role of microbial symbionts in promoting host resilience to climate change.

Author affiliations: ^aDepartment of BioSciences, Rice University, Houston, TX, 77005; ^bDepartment of Biology, University of Miami, Miami, FL, 33146; ^cDepartment of Biology, University of New Mexico, Albuquerque, NM, 87131

J.C.F. contributed to data collection, data analysis, and led manuscript drafting. S.Z. contributed to data collection and manuscript revisions. K.D.W. contributed to research conception, data collection, and manuscript revisions. J.A.R. established transplant plots, contributed to research conception, data collection, and manuscript revisions. T.E.X.M. contributed to research conception, data collection, data analysis, and manuscript revisions.

The authors declare no conflict of interest

¹To whom correspondence should be addressed. E-mail: jcf221@miami.edu

enemies (21, 22). Some of the best studied examples include bacterial symbionts of aphids and other insects that provide their hosts with thermal tolerance through the production of heat-shock proteins (23), and plant-fungal symbionts that produce anti-herbivore toxins (24–26). However, these diverse protective symbioses are context-dependent: the magnitude of benefits depends on environmental or biotic conditions (27) and thus will vary temporally in a stochastic environment (28). We hypothesized that context-dependent benefits from symbionts may buffer hosts against variability through strong benefits during harsh periods, and neutral or even costly outcomes during benign periods, reducing the impacts of host exposure to extremes and dampening inter-annual variance relative to non-symbiotic hosts. Variance buffering is a previously unexplored mechanism by which symbionts may benefit their hosts in addition to elevating average fitness, the focus of most previous research.

We tested the hypothesis that context-dependent benefits of symbiosis buffer hosts from the fitness costs of environmental variability using data from taxonomically replicated, long-term symbiont-removal experiments. We (i) quantified the effects of symbiosis on the mean and variance of host vital rates (survival, growth and reproduction), (ii) investigated the relationship between host life history traits and the magnitude of symbiont-mediated variance buffering, (iii) evaluated the relative contribution of mean and variance effects to long-term population growth rates (λ_s), and (iv) projected the consequences of symbiont-mediated variance buffering under increased environmental variability.

Results and Discussion

Our experiment began in 2007 with seven grass species that host *Epichloë* fungal endophytes. Located in south-central Indiana, USA, the experiment consisted of annually censused populations founded with either naturally symbiotic plants (S+) or those that had their symbionts experimentally removed via a heat treatment (S-) (See Materials and Methods for a full list of species and experimental methods). *Epichloë* endophytes are specialized symbionts growing intercellularly in the aboveground tissue of ~30% of cool-season (C_3) grass species (29). These fungi are primarily transmitted vertically from maternal plants through seeds (30). They produce a variety of alkaloids that can protect host plants from herbivory (31) and drought stress (32).

The unique data from this long-term experiment are distinctly suitable for detecting fitness benefits of microbial symbioses that arise through variance buffering. We collected annual demographic data on the survival, growth, reproduction, and recruitment of all plants within replicated S+ and S- plots, which on average had 13.3 individuals/ m^2 over the course of the experiment. Each census year was a sample of inter-annual climatic variation ($n = 14$ years; comprising 13 demographic transition years). We fit hierarchical Bayesian generalized linear mixed models to the vital rate data using RStan (33), which allowed us to isolate endophyte effects on vital rate means and variances, borrow strength across species for some variance components, and propagate uncertainty from the individual-level vital rates to population projection models (34). The projection models were stochastic matrix population models parameterized for each host species from the vital rate regressions to quantify endophyte effects on

stochastic population growth rates (λ_s) and decompose the overall effect of the symbiosis into contributions through mean vital rates, variance in vital rates, and their interaction (Methods section describes the statistical methods in full).

Quantifying symbiont mediated variance buffering. Across seven host species, eight vital rates, 14 years, and 16,789 individual plants, our analysis provides the first empirical support for the hypothesis of symbiont mediated variance buffering. Endophytes reduced inter-annual variance for 66% (37/56) of host species-vital rate combinations (average Cohen's D for effects on vital rate standard deviation: -0.15) (Fig. 1A). Endophytes also increased mean vital rates for the majority (36/56) of host species-vital rate combos (average Cohen's D for effects on vital rate mean: 0.15), and benefits were particularly strong for host survival, plant growth and germination (Fig. 1A). The relative magnitude of symbiont effects on means versus variances differed among host species and their vital rates. For example, endophytes modestly increased mean adult survival (Fig. 1C) and reduced variance in survival (Fig. 1D) for *Festuca subverticillata*, while for *Poa alsodes*, variance buffering was more apparent in seedling growth and inflorescence production (Fig 1E). Interestingly, certain vital rates showed costs of endophyte symbiosis. Symbiotic individuals of *A. perennans* grew larger than those without endophytes (Fig. 1B), yet endophytes also reduced this species' mean germination rates (Fig. 1A). Similarly, endophyte symbiosis increased variance in seedling growth for *Elymus villosus* and *Festuca subverticillata* (Fig. 1A).

Because not all vital rates contribute equally to fitness, we used stochastic matrix models to integrate the diverse effects on vital rates described above into comprehensive measures for the mean and variance of fitness. On average across host species, endophyte-symbiotic populations had greater mean fitness (> 92% confidence that endophytes increased $\bar{\lambda}$) and lower inter-annual variability in fitness (> 86% confidence that endophytes decreased the coefficient of variation of λ) than endophyte-free populations (Fig. 2). For some host species, the CV of λ was reduced by as much as 170% (*P. alsodes*, *F. subverticillata*), while for others, endophyte effects on variance were substantially smaller (6% lower for *E. villosus*, 16% lower for *A. perennans*), or even positive (27% increase for *E. virginicus*). When mean and variance effects of symbionts were considered together, none of the host-symbiont pairings were antagonistic (i.e., with endophytes that both decreased mean fitness and increased variance) (Fig. 2C), suggesting that variation across host species and vital rates in mean and variance effects may reflect alternative strategies that yield similar benefits of endophyte symbiosis.

Reduced sensitivity to drought, as has been reported for some *Epichloë* symbioses (32), is a candidate mechanism that could generate a signature of variance buffering. Accordingly, analysis of climate-explicit population models indicated that for five of seven taxa, symbiotic populations were less sensitive to annual or growing season drought (12-month or 3- month drought index; Standardized Precipitation-Evapotranspiration Index (35)) than symbiont-free populations (Supporting Information Text; Fig. S24-S25; Table S3). However, we did not find a strong relationship between the magnitude of variance buffering and relative drought sensitivities, suggesting that other climatic factors or other

249 aspects of the abiotic or biotic environment may elicit benefits
250 of endophyte symbiosis, including documented resistance
251 to herbivory for six of the taxa (36, 37). Identifying the
252 potentially complex relationships between vital rates and
253 environmental drivers remains a key challenge for accurate
254 forecasts of the ecological impacts of environmental stochasticity
255 (38).

256 **Life history analysis.** Long-lived species, those on the slow
257 end of the slow-fast life history continuum, are expected
258 to be less sensitive to environmental variability (39), a
259 pattern which has empirical support across plants (40) and
260 animals (8, 41). Therefore, we predicted that host species
261 with long lifespans that produce few, large offspring would
262 benefit less from the variance buffering effects of endophytes
263 than species with fast life cycles that produce many smaller
264 offspring with low per-capita chance of success (42, 43).
265 In support of this prediction, symbionta with trait values
266 representing faster life history strategies experienced greater
267 variance buffering from endophytes than those with slow
268 life histories (Fig. 3). Bayesian phylogenetic mixed-effects
269 models, controlling for species' relatedness, indicated that
270 variance buffering was stronger for host species with shorter
271 lifespan (Fig. 3A; 75% probability of positive relationship
272 with empirically observed max age) and smaller seeds (Fig.
273 3B; 73% probability of positive relationship with seed length).
274 Other life history traits similarly had positive but weaker
275 support for the prediction that faster life history traits would
276 correlate with stronger variance buffering (Fig. S26-S28).
277 Additionally, the three host species for which the overall
278 mutualism was weakest (*Elymus villosus*, *Elymus virginicus*,
279 and *Poa sylvestris*) (Fig. 2C) were the only hosts for which
280 we observed fungal stromata, fruiting bodies capable of
281 horizontal (contagious) transmission (Table S2), in line with
282 theoretical expectations for strict vertical transmission driving
283 the evolution of strong host-symbiont mutualisms (20, 44).
284 Conclusions about life histories are somewhat constrained by
285 the narrow range of trait values among these closely related
286 species in the grass sub-family Pooideae. Our understanding of
287 how life history variation modulates the fitness consequences
288 of microbial symbiosis would profit from tests across a wide
289 span of taxonomic groups (45).

290 **Relative contributions of mean and variance effects.** To
291 evaluate the relative importance of mean fitness benefits
292 and variance buffering as alternative pathways of mutualism,
293 we decomposed the overall effect of the symbiosis on λ_s
294 using stochastic simulations of four versions of population
295 models that included both mean and variance buffering effects,
296 mean effects alone, variance effects alone, or neither mean
297 nor variance effects. Overall, the full effect of symbiosis on
298 λ_s , averaged across host species, provided strong evidence of
299 grass-endophyte mutualism (100% certainty of a positive total
300 effect on λ_s) (Fig. 4; see Fig. S21 for individual host species).
301 Contributions to this total effect derived from both mean
302 and variance buffering effects, as well as a slightly negative
303 interaction (i.e., the combined influence of mean and variance
304 effects was lower than the sum of their individual effects).
305 Endophytes' contributions to the stochastic growth rate (λ_s)
306 from mean effects were four times greater, averaged across
307 species, than contributions from variance buffering (Fig. 4),
308 suggesting that, under the regime of environmental variability

311 represented by our 14-year study, dampened fluctuation in
312 fitness is a far less important element of the benefits of
313 symbiosis than elevated mean fitness.

314 **Consequences of variance buffering under increased environmental variability.** Simulations of increased environmental
315 variability, a key prediction of climate change forecasts (2),
316 indicated that mutualism with microbial symbionts, and
317 their variance buffering effects in particular, will take on
318 increased importance for grasses in a more variable future
319 climate. To simulate increased variability, we repeated
320 the decomposition of λ_s under two additional scenarios,
321 randomly sampling transition matrices from either the six
322 or two most extreme years experienced by each species,
323 subsets of the thirteen transition matrices across the study
324 period. The six- and two-years scenarios increased the
325 standard deviation of yearly growth rates by 1.3 and 2.1
326 times, respectively, relative to the ambient scenario without
327 changing mean growth rates (< 2.3% difference between
328 simulation treatments)(See SM; Fig. S21-22). Increased
329 variability elicited stronger mutualistic benefits of endophyte
330 symbiosis (Fig. 3) than ambient variability (overall effect
331 of the symbiosis increased by > 130%). This increase was
332 driven by increased contributions from the variance buffering
333 mechanism (from a 24% contribution in the ambient scenario
334 to a 66% contribution in the most variable scenario). In the
335 most variable scenario, the relative importance of mean and
336 variance effects reverses, with variance buffering contributions
337 that are 1.5 times greater than contributions from mean
338 benefits, averaged across species (Fig. 4). Thus, variance
339 buffering – a cryptic microbial influence that manifests over
340 long temporal scales – is poised to become the dominant
341 way in which grasses benefit from symbiosis with fungal
342 endophytes in future climates.

343 Ecologists increasingly recognize the importance of symbiotic
344 microbes for host organisms and the populations,
345 communities, and ecosystems in which their hosts reside (46–
346 49). Despite awareness of these ubiquitous interactions, long-
347 term studies of microbial symbiosis are very rare. Our analysis
348 of replicated 14-year field experiments manipulating the
349 presence/absence of fungal symbionts in plants demonstrated
350 for the first time that heritable microbes can commonly
351 benefit hosts not only through improved mean fitness – the
352 focus of most previous research – but also via buffering against
353 environmental variance. Our results provide an important
354 advance to improve forecasts of the responses of populations
355 (and symbionta) to increasing environmental stochasticity
356 under global change, suggesting that, for some species,
357 microbial symbiosis may compensate for the lack of intrinsic
358 tolerance of variability conferred by “slow” life history traits.
359 We found that symbiont-mediated variance buffering made
360 relatively weak contributions to host-symbiont mutualism
361 under the current regime of environmental variability, but is
362 likely to become the dominant benefit that fungal endophytes
363 confer to grass hosts in more variable future environments.
364 This result emerges from the context-dependent nature of
365 grass-endophyte interactions, combined with the observation
366 that environmental stochasticity generates fluctuation in
367 context. These key ingredients, and thus the potential for
368 symbiont-mediated variance buffering, similarly apply to the
369 diverse host-microbe symbioses across the tree of life.

373 **Materials and Methods**

374
375
376 **Study site and species.** This study was conducted at Indiana University's Lilly-Dickey Woods (39.238533, -86.218150) in Brown County, Indiana, USA. This site is part of the Eastern broadleaf forests of southern Indiana, where the ranges of many understory cool-season grass species overlap. The experiment focused on seven of these grasses which host *Epichloë* endophytes (*Agrostis perennans*, *Elymus villosus*, *Elymus virginicus*, *Festuca subverticillata*, *Lolium arundinaceum*, *Poa alsodes*, and *Poa sylvestris*) (Table S1).

383 **Endophyte removal, plant propagation, and field set-up.** Seeds from
384 naturally symbiotic populations of the seven focal host species
385 were collected during summer-fall 2006 from Lilly-Dickey Woods
386 in Brown County, Indiana, USA, and the nearby Bayles Road
387 Teaching and Research Preserve (39.220167, -86.542683). To
388 generate symbiotic (S+) and symbiont-free (S-) plants from the
389 same genetic lineages, seeds from each species were disinfected
390 with a heat treatment described in Table S1 or left untreated. The
391 heat treatment created symbiont-free plants by warming seeds to
392 temperatures at which the fungus becomes inviable but the host
393 seeds can still germinate. Both heat-treated and untreated seeds
394 were surface sterilized with bleach to remove epiphyllous microbes,
395 cold stratified for up to 4 weeks, then germinated in a growth
396 chamber before transfer to the greenhouse at Indiana University
397 where they grew for ~ 8 weeks. We confirmed endophyte status
398 by staining thin sections of inner leaf sheath with aniline blue and
399 examining tissue for fungal hyphae at 200X magnification (50).
400 We established the field plots with vegetatively propagated clones
401 of similar sizes. By starting the experiment with plants of similar
402 sizes and the same number of unique genotypes, we aimed to limit
403 any potential effects of heat treatments on initial plant growth
(51).

404 During the fall of 2007 and spring of 2008, we established
405 10 3x3 m. plots for *A. perennans*, *E. villosus*, *E. virginicus*, *F.*
406 *subverticillata*, and *L. arundinaceum* and 18 plots for *P. alsodes*
407 and *P. sylvestris*. Half of the plots were randomly assigned to
408 be planted with either symbiotic (S+) or with symbiont-free (S-)
409 plants, and initiated with 20 evenly spaced S+ or S- individuals
410 labeled with aluminum tags. In spring 2008, we placed plastic
411 deer net fencing around each plot to limit deer herbivory and
412 disturbance; damaged fences were regularly replaced.

413 **Long-term demographic data collection.** Each summer starting in
414 2008 through 2021, we censused all individuals in each plot for
415 survival, growth and reproduction, adding new recruits to the
416 census. We censused each species during its peak fruiting stage
417 (May: *Poa alsodes*, *Poa sylvestris*; June: *Festuca subverticillata*;
418 July: *Elymus villosus*, *Elymus virginicus*, *Lolium arundinaceum*;
419 September: *Agrostis perennans*), such that the censuses were pre-
420 breeding and new recruits came from the previous years' seed
421 production. Leaf litter was cleared out of each plot prior to the
422 census, to aid in locating plants. For each plant remaining from
423 the previous year, we determined survival, measured its size as
424 a count of the number of tillers, and collected reproductive data
425 as counts of the number of reproductive tillers and counts of the
426 number of seed-bearing spikelets on all reproductive tillers to a
427 maximum of three. We also tagged all unmarked individuals that
428 were recruits from the previous years' seed production and collected
429 the same demographic data. New recruits typically had one tiller
430 and were non-reproductive. In 2008 and 2009, we took additional
431 counts of seeds per inflorescence for all reproducing individuals in
432 the plots to ground-truth our subsample estimates. For *Agrostis*
433 *perennans*, we also collected seed counts in 2010. In 2018, we
434 stopped collecting data for the *Lolium arundinaceum* plots, which
435 had very high survival and low recruitment, and consequently very
436 low variation across years. For each individual in the experiment,
437 our data record their transitions in size and reproduction from one
438 year to the next. In total across 14 years, the dataset includes
439 demographic information for 16,789 individual host-plants and
440 31,216 transition-year observations.

441 We expected plots to maintain their endophyte status (S+ or
442 S-) because the fungal symbionts are almost exclusively vertically
443 transmitted, and plots were spaced a minimum of 5 m apart,
444 limiting seed dispersal or horizontal transmission of the symbiont
445 between plots. However, we regularly confirmed endophyte treat-
446 ment throughout the lifetime of the experiment by opportunistically
447 taking subsets of seeds from reproductive individuals and scoring
448 them for their endophyte status with microscopy as above. Overall,
449 these scores reflected 98% faithfulness of recruits to their expected
450 endophyte status across species and plots (Fig. S23; Supplement
451 data). Additionally, we have rarely observed fungal stromata,
452 the fruiting bodies by which *Epichloë* are potentially transmitted
453 horizontally, provided the fly vector is also present (52). For *A.*
454 *perennans*, *F. subverticillata*, *L. arundinaceum*, and *P. alsodes*, we
455 never observed stromata. We observed stromata only infrequently
456 for *E. villosus*, and even more rarely for *E. virginicus* and *P.*
457 *sylvestris* (Table S2). For these species, stromata have only
458 been observed on 35, 4, and 6 plants respectively, making up
459 < 0.3% of all censused plants (Supplemental data). These stromata
460 observations occurred irregularly across years; in most years there
461 were no stromata during the census, and in a few years several
462 plants produced stromata.

463 **Vital rate modeling.** Equipped with these demographic data, we
464 fit statistical models for survival, growth, flowering (yes or no),
465 fertility of flowering plants (number of flowering tillers), production
466 of seed-bearing spikelets (number per inflorescence), the average
467 number of seeds per spikelet, and the recruitment of seedlings from
468 the preceding year's seed production (Fig. S1 - S10). We fit these
469 vital rates as generalized linear mixed models in a hierarchical
470 Bayesian framework using RStan (33). All vital rate models
471 included random plot and year effects, with separate estimates of
472 year-to-year variance for symbiotic and symbiont-free plants, to
473 quantify the effect of endophytes on inter-annual variance (Fig.
474 S11 - S18). These variance components and other predictors as
475 described below were given vague priors (53). We ran each vital
476 rate model for 2500 warm-up and 2500 MCMC sampling iterations
477 with three chains. We assessed model convergence with trace
478 plots of posterior chains and checked for \hat{R} values less than 1.01,
479 indicating low within- and between-chain variation (54, 55). For
480 those models that showed poor convergence, we extended the
481 MCMC sampling to include 5000 warm-up and 5000 sampling
482 iterations, which was only necessary for seedling growth. We
483 graphically checked vital rate model fit with posterior predictive
484 checks comparing simulated data from 500 posterior draws with
485 the observed data (Fig. S19-S20).

486 **Survival** - We modeled survival as a Bernoulli process, where
487 the survival (S) of an individual i in plot p and census year t was
488 predicted by the plot-level endophyte status (e), host species (h),
489 size in the preceding census, and the plant's origin status (whether
490 it was initially transplanted or naturally recruited into the plot).

$$\begin{aligned} S_{i,p(e),h,t} &\sim \text{Bernoulli}(\hat{S}_{i,p(e),h,t}) & [2a] \\ \text{logit}(\hat{S}_{i,p(e),h,t}) &= \beta_{0h} + \beta_1 * \text{origin}_i & [2b] \\ &+ \beta_{2h} * \text{endo}_i + \beta_{3h} * \text{size}_{i,t-1} + \tau_{e,h,t} + \rho_p & [2c] \\ \tau_{e,h,t} &\sim \text{Normal}(0, \sigma_{\tau_{e,h}}^2) & [2d] \\ \rho_p &\sim \text{Normal}(0, \sigma_p^2) & [2e] \end{aligned}$$

491 Here, \hat{S} is the survival probability ($p(e)$ indicates that plot
492 identity is uniquely associated with an endophyte status), β_{0h}
493 is an intercept specific to each host species, β_1 is the effect of
494 the plant's recruitment origin, β_{2h} is the endophyte effect, β_{3h}
495 is the size effect, $\tau_{e,h,t}$ is a normally distributed year effect for
496 each species and endophyte status with variance $\sigma_{\tau_{e,h}}^2$, and ρ_p is a
497 normally distributed plot effect with variance σ_p^2 . We assume that
498 origin effect β_1 and plot-to-plot variance σ_p^2 are shared across host
499 species, allowing us to "borrow strength" across the multi-species
500 dataset; other model parameters are unique to host species. We
501 separately modeled the survival of newly recruited seedlings, which
502 were typically one tiller and non-reproductive, with a similar model
503 but omitting size dependence and the effect of the plant's origin
504 status. All random effects were estimated independently between
505 seedling and adult vital rates models.

497 *Growth* - We modeled plant size in census year t (G) with
 498 the same linear predictor for the mean as described for survival.
 499 Because we measured size as positive integer-valued counts of tillers,
 500 we modeled it with a zero-truncated Poisson-inverse Gaussian
 501 distribution. This distribution includes a shape parameter λ_G to
 502 account for overdispersion in the data. We additionally modeled
 503 the growth of newly recruited seedlings separately with a Poisson-
 504 inverse Gaussian model omitting size structure and the plants'
 505 origin status as with seedling survival.

506 *Flowering* - We modeled whether or not a plant was flowering
 507 during the census (P) as a Bernoulli process, with the same linear
 508 predictor for the mean as described above for survival except that
 509 size dependence for reproductive vital rates was determined by the
 510 individual's size during the same census year as opposed to its size
 511 during the previous year.

512 *Fertility* - For a plant that was flowering during the census,
 513 its fertility was the number of reproductive tillers produced (F),
 514 which we modeled as a function of size in the same census period
 515 with a zero-truncated Poisson-Inverse Gaussian distribution, with
 516 the same linear predictor for the mean as described above.

517 *Spikelets per Inflorescence* - Spikelet production (K) was
 518 recorded as integer counts on up to three inflorescences per
 519 reproducing plant. We modeled these data with a negative
 520 binomial distribution, with the same linear predictor for the mean
 521 as described above.

522 *Seed Production per Spikelet* - For individuals with recorded
 523 counts of seeds production, we calculated the number of seeds per
 524 spikelet from our counts of seeds and spikelets per inflorescence,
 525 and then modeled seeds per spikelet (D) as normally distributed
 526 averages for each species and endophyte status. Because we had
 527 less detailed data across years and plants for seed production than
 528 for other reproductive vital rates, we omitted both plot and year
 529 random effects.

530 *Seedling Recruitment* - We used a binomial distribution to
 531 model the recruitment of new seedlings (R) into the plots from seeds
 532 produced in the preceding year, assuming no long-lived seed
 533 bank. We included an intercept specific to each host and endophyte
 534 status and the same random effects structure as in other models.
 535 We estimated the number of seeds per plot in the preceding year
 536 by multiplying the total number of reproductive tillers per plant
 537 by the mean number of spikelets per inflorescence on that plant
 538 and by a sample from the posterior distribution of mean number
 539 of seeds per spikelet (D). For plants with missing fertility or
 540 spikelet data, we used the expected number of reproductive tillers
 541 (F) or of spikelets per inflorescence from (K), drawing from the
 542 full posteriors of our models. We rounded this value to get the
 543 estimated seed production for each individual, and finally summed
 544 across all reproductive plants in each year and plot to get the total
 545 number of seeds produced.

546 **Stochastic population model.** Using the fitted vital rate models, we
 547 parameterized stochastic matrix projection models including two
 548 state variables: r_t (the number of newly recruited individuals in
 549 year t), and n_t (a vector including all non-seedling individuals in
 550 year t), and n_t^x (the x^{th} element of n_t , ranging from one to the maximum number
 551 of tillers U). We used the same model structure for each species
 552 and endophyte status (not shown in model notation). The total
 553 number of recruits in year $t + 1$ is given by:

$$554 r_{t+1} = \sum_{x=1}^U P(x; \boldsymbol{\tau}_P) F(x; \boldsymbol{\tau}_F) K(x; \boldsymbol{\tau}_K) DR(\boldsymbol{\tau}_R) n_t^x \quad [3]$$

555 The total number of seeds produced by a maternal plant of size
 556 x is the product of the size-specific probability of flowering P ,
 557 the number of reproductive tillers F , the number of spikelets
 558 per inflorescence K , and the number of seeds per spikelet D .
 559 Multiplying by the probability of transitioning from seed to seedling
 560 R gives a per-capita rate of seedling production, which is multiplied
 561 by the number of plants of size x (n_t^x , the x^{th} element of n_t)
 562 and summed. Each function also depends on the species- and
 563 endophyte-specific year random effects for that vital rate ($\boldsymbol{\tau}$, a
 564 vector of year-specific values derived from the statistical models).

565 Recruitment, survival and growth determine the rest of the
 566 population dynamics of the new seedlings and larger plants. The

567 number of y -sized plants in year $t + 1$ is given by:

$$568 n_{t+1}^y = Z(y; \boldsymbol{\tau}_Z) B(\boldsymbol{\tau}_B) r_t + \sum_{x=0}^U S(x; \boldsymbol{\tau}_S) G(x, y; \boldsymbol{\tau}_G) n_t^x \quad [4]$$

569 where n_{t+1}^y is the y^{th} element of vector n_{t+1} . The first term on
 570 the right hand side of Eqn. 4 represents growth (Z) and survival
 571 (B) of seedling recruits. The second term includes the survival
 572 of x -sized plants and the growth of survivors from size x to y ,
 573 summed over all x . To avoid predictions of unrealistic growth
 574 outside of the observed size distribution, we set a ceiling on the
 575 growth function for plants at the 97.5th percentile in the observed
 576 size distribution (56). Each of the functions in Eqns. 3 and 4
 577 have separate intercepts and year random effects for symbiotic and
 578 symbiont-free populations, allowing us to calculate the effect of
 579 endophyte symbiosis on the mean and variance of λ , the dominant
 580 eigenvalue of the projection matrix. Analysis of climate-explicit
 581 population models followed the same logic as for the climate-
 582 implicit models presented here with the addition of parameters
 583 defining the relationship between either annual or growing season
 584 drought index and each vital rate. A full description of climate-
 585 explicit methods can be found in the Supporting Information Text.

586 **Life History Analysis.** We collected metrics describing each host
 587 species' life history to test the relationship between pace of life and
 588 variance buffering (Table S1). Using the Rage package (57), we
 589 calculated R_0 , longevity, and generation time from our estimated
 590 transition matrices using the S- mean matrix as the reference
 591 condition. We recorded seed length measurements as the average
 592 lemma length from the Flora of North America (58). We also
 593 calculated and the 99th percentile of maximum observed age for
 594 each species from their S- populations. Next, we fit Bayesian
 595 phylogenetic mixed-effects models using the 'brms' package (59)
 596 to test the relationship between each life history trait and the
 597 estimated effect of symbiosis on the coefficient of variation from
 598 the population model while controlling for phylogenetic non-
 599 independence in the hosts (Fig. 26) and the symbiont (Fig.
 600 S27). We pruned larger species-level phylogenies of plants(60) and
 601 *Epichloë* fungi (61) to include the focal species. *Agrostis perennans*
 602 was not included in the tree, and so we used a congeneric species,
 603 *A. hyemalis*. We defined separate phylogenetic covariance matrices
 604 for each pruned tree. We propagated uncertainty in the estimated
 605 variance buffering effect with a measurement error model. Thus
 606 the model for the variance buffering effect V was given by:

$$597 V_{MEAN,h} \sim Normal(V_{EST,h}, V_{SD,h}) \quad [5a]$$

$$598 V_{EST,h} \sim Normal(\mu_h, \sigma) \quad [5b]$$

$$599 \mu = \alpha + \beta * trait + \pi \quad [5c]$$

$$600 \alpha \sim Normal(0, .5) \quad [5d]$$

$$601 \beta \sim Normal(0, .1) \quad [5e]$$

$$602 \sigma \sim Half-Normal(.044, .01) \quad [5f]$$

$$603 \pi \sim Normal(0, \sigma_\pi * \mathbf{A}) \quad [5g]$$

$$604 \sigma_\pi \sim Half-Normal(0, .1) \quad [5h]$$

605 Here, V_{EST} is the variance buffering effect for each host species
 606 h , estimated from the posterior mean (V_{MEAN}) and standard
 607 deviation (V_{SD}), propagating uncertainty associated with the
 608 effect of symbiosis in our population model. The model includes
 609 an intercept parameter (α) and a slope parameter (β) defining
 610 the relationship between the variance buffering effect and the
 611 life history trait. The residual standard deviation is given by
 612 (σ). We used weakly informative priors to aid model convergence.
 613 Each prior was centered at zero, except for the residual standard
 614 deviation, which we centered at the standard deviation of the
 615 estimated variance buffering effect, .04. The phylogenetic random
 616 effect (π) has a standard deviation (σ_π) which is structured by
 617 the covariance matrix \mathbf{A} . We ran each MCMC sampling chain for
 618 8000 warmup iterations and 2000 sampling iterations. We assessed
 619 model convergence as described for the vital rate models.

620 **Mean-variance decomposition.** To calculate stochastic population
 621 growth rates (λ_s) for each host species and endophyte status

we simulated population dynamics for 1000 years by randomly sampling from the 13 annual transition matrices observed over the course of the experiment, discarding the first 100 years to minimize the influence of initial conditions. Sampling observed transition matrices produces models which realistically capture inter-annual variation by preserving correlations between vital rates (62). We tallied the total population size at each time step as $N_t = r_t + \sum_{x=1}^U n_t^x$ and calculated the stochastic growth rate as $\log(\lambda_s) = E[\log(\frac{N_t}{N_{t+1}})]$ (63, 64). We calculated the total effect of endophyte symbiosis as the difference in λ_s between S+ and S- populations. We propagated uncertainty from the vital rate models to the calculation of λ_s using 500 draws from the posterior distribution of model parameters.

We decomposed the total endophyte effect on λ_s into contributions from effects on vital rate means, variances, and their interaction. Specifically, we repeated the calculation of λ_s for two additional “treatments”: (1) endophyte effects on mean vital rates only, with inter-annual variances shared between S+ and S- at the S- reference level for all vital rates, and (2) endophyte effects on vital rate variances only, with vital rate means shared between S+ and S- at the S- reference level. The combination of all four λ_s treatments (S+ vital rate means and variances, S- means and variances, S+ means with S- variances, S- means with S+ variances) allowed us to quantify to what extent the overall effect of symbiosis derives from changes in vital rates means, variances, and their interaction. The interaction occurs because the variance penalty to stochastic growth is proportional to the mean value of annual growth rates (see Eq. 1) such that variance is more detrimental for populations with low average growth rates. For

each contribution element (variance buffering, mean effects, and their interaction), we calculated a cross species mean to assess the overall contributions (Fig. 4).

Simulation experiment. To create scenarios of increased variance relative to that observed during the study period, we repeated the stochastic growth rate estimation and decomposition, but sampling only a subset of the 13 observed annual transition matrices. We created two scenarios of increased environmental variance by sampling the transition matrices associated with the six or two most extreme λ values, representing the six or two best and worst years, using S- populations as the reference condition. By sampling away from an average year in both directions, the mean value of annual growth rates remained similar across treatments ($\bar{\lambda}$ averaged across species: All years = 0.71; 6 years = 0.71; 2 years = 0.73; Fig. S21A), while the standard deviation more than doubled ($sd(\lambda)$ averaged across species: All years = 0.25; 6 years = 0.34; 2 years = 0.54 ; Fig. S21B), representing elevated environmental fluctuations. We performed the same mean-variance decomposition for these scenarios as for the ambient conditions (all 13 years sampled) for all host species described above (Fig. S22).

ACKNOWLEDGMENTS. We thank Mark Sheehan, Ali Campbell, Kyle Dickens, Blaise Willis, and Sar Lindner for contributions to field data collection. We also thank Volker Rudolf, Daniel Kowal, Lydia Beaudrot and Judie Bronstein for helpful comments on and discussion of this project. This research was supported by the National Science Foundation (Grants 1754468 and 2208857).

1. S Seneviratne, et al., *Changes in climate extremes and their impacts on the natural physical environment*. (Cambridge University Press), (2012).
2. IPCC, Climate change 2021: The physical science basis (2021).
3. RC Lewontin, D Cohen, On Population Growth in a Randomly Varying Environment. *Proc. Natl. Acad. Sci.* **62**, 1056–1060 (1969) Publisher: National Academy of Sciences Section: Biological Sciences: Zoology.
4. SD Tuljapurkar, Population dynamics in variable environments. III. Evolutionary dynamics of r-selection. *Theor. Popul. Biol.* **21**, 141–165 (1982).
5. JE Cohen, Comparative statics and stochastic dynamics of age-structured populations. *Theor. population biology* **16**, 159–171 (1979).
6. S Tuljapurkar, *Population dynamics in variable environments*. (Springer Science & Business Media) Vol. 85, (2013).
7. CA Pfister, Patterns of variance in stage-structured populations: evolutionary predictions and ecological implications. *Proc. Natl. Acad. Sci.* **95**, 213–218 (1998).
8. WF Morris, et al., Longevity can buffer plant and animal populations against changing climatic variability. *Ecology* **89**, 19–25 (2008).
9. A Compagnoni, et al., The effect of demographic correlations on the stochastic population dynamics of perennial plants. *Ecol. Monogr.* **86**, 480–494 (2016).
10. MM Ellis, EE Crone, The role of transient dynamics in stochastic population growth for nine perennial plants. *Ecology* **94**, 1681–1686 (2013).
11. RC Rodríguez-Caro, et al., The limits of demographic buffering in coping with environmental variation. *Oikos* **130**, 1346–1358 (2021).
12. S Tuljapurkar, SH Orzack, Population dynamics in variable environments i. long-run growth rates and extinction. *Theor. Popul. Biol.* **18**, 314–342 (1980).
13. J Fieberg, SP Ellner, Stochastic matrix models for conservation and management: a comparative review of methods. *Ecol. letters* **4**, 244–266 (2001).
14. ES Menges, Applications of population viability analyses in plant conservation. *Ecol. Bull.* pp. 73–84 (2000).
15. A Kuparinen, A Boit, FS Valdovinos, H Lassaux, ND Martinez, Fishing-induced life-history changes degrade and destabilize harvested ecosystems. *Sci. reports* **6**, 22245 (2016).
16. CH Hilde, et al., The Demographic Buffering Hypothesis: Evidence and Challenges. *Trends Ecol. & Evol.* **0** (2020) Publisher: Elsevier.
17. R Rodriguez, J Whit Jr, AE Arnold, aRa Redman, Fungal endophytes: diversity and functional roles. *New phytologist* **182**, 314–330 (2009).
18. M McFall-Ngai, et al., Animals in a bacterial world, a new imperative for the life sciences. *Proc. Natl. Acad. Sci.* **110**, 3229–3236 (2013).
19. LJ Funkhouser, SR Bordestein, Mom knows best: the universality of maternal microbial transmission. *PLoS biology* **11**, e1001631 (2013).
20. PE Fine, Vectors and vertical transmission: an epidemiologic perspective. *Annals New York Acad. Sci.* **266**, 173–194 (1975).
21. JA Russell, NA Moran, Costs and benefits of symbiont infection in aphids: variation among symbionts and across temperatures. *Proc. Royal Soc. B: Biol. Sci.* **273**, 603–610 (2006).
22. SN Kirlin, SM Emery, JA Rudgers, Fungal symbionts alter plant responses to global change. *Am. J. Bot.* **100**, 1445–1457 (2013).
23. HE Dunbar, ACC Wilson, NR Ferguson, NA Moran, Aphid thermal tolerance is governed by a point mutation in bacterial symbionts. *PLoS biology* **5**, e96 (2007).
24. R Reyna, P Cooke, D Grum, D Cook, R Creamer, Detection and localization of the endophyte undifilum oxytropis in locoweed tissues. *Botany* **90**, 1229–1236 (2012).
25. K Saikkonen, PE Gundel, M Helander, Chemical ecology mediated by fungal endophytes in grasses. *J. chemical ecology* **39**, 962–968 (2013).
26. M Neyaz, DR Gardner, R Creamer, D Cook, Localization of the swainsonine-producing chaetothyriales symbiont in the seed and shoot apical meristem in its host ipomoea carnea. *Microorganisms* **10**, 545 (2022).
27. SA Chamberlain, JL Bronstein, JA Rudgers, How context dependent are species interactions? *Ecol. letters* **17**, 881–890 (2014).
28. P Jordano, Spatial and temporal variation in the avian-frugivore assemblage of prunus mahaleb: patterns and consequences. *Oikos* pp. 479–491 (1994).
29. A Leuchtmann, Systematics, distribution, and host specificity of grass endophytes. *Nat. toxins* **1**, 150–162 (1992).
30. GP Cheplick, S Faeth, SH Faeth, *Ecology and evolution of the grass-endophyte symbiosis*. (OUP USA), (2009).
31. D Brem, A Leuchtmann, Epichloë grass endophytes increase herbivore resistance in the woodland grass brachypodium sylvaticum. *Oecologia* **126**, 522–530 (2001).
32. FA Decunta, LI Pérez, DP Malinowski, MA Molina-Montenegro, PE Gundel, A systematic review on the effects of epichloë fungal endophytes on drought tolerance in cool-season grasses. *Front. plant science* **12**, 644731 (2021).
33. Stan Development Team, RStan: the R interface to Stan (2022) R package version 2.21.7.
34. BD Elderd, TE Miller, Quantifying demographic uncertainty: Bayesian methods for integral projection models. *Ecol. Monogr.* **86**, 125–144 (2016).
35. SM Vicente-Serrano, S Beguería, JL López-Moreno, A multiscale drought index sensitive to global warming: the standardized precipitation evapotranspiration index. *J. climate* **23**, 1696–1718 (2010).
36. JA Rudgers, K Clay, An invasive plant-fungal mutualism reduces arthropod diversity. *Ecol. Lett.* **11**, 831–840 (2008).
37. CM Crawford, JM Land, JA Rudgers, Fungal endophytes of native grasses decrease insect herbivore preference and performance. *Oecologia* **164**, 431–444 (2010).
38. J Ehrlén, WF Morris, Predicting changes in the distribution and abundance of species under environmental change. *Ecol. letters* **18**, 303–314 (2015).
39. GI Murphy, Pattern in life history and the environment. *The Am. Nat.* **102**, 391–403 (1968).
40. A Compagnoni, et al., Herbaceous perennial plants with short generation time have stronger responses to climate anomalies than those with longer generation time. *Nat. communications* **12**, 1–8 (2021).
41. C Le Coeur, NG Yoccoz, R Salguero-Gómez, Y Vindenes, Life history adaptations to fluctuating environments: Combined effects of demographic buffering and lability. *Ecol. Lett.* **25**, 2107–2119 (2022).
42. M Rees, Evolutionary ecology of seed dormancy and seed size. *Philos. Transactions Royal Soc. London. Ser. B: Biol. Sci.* **351**, 1299–1308 (1996).
43. AT Moles, M Westoby, Seedling survival and seed size: a synthesis of the literature. *J. Ecol.* **92**, 372–383 (2004).
44. ME Afkhami, JA Rudgers, Symbiosis lost: imperfect vertical transmission of fungal endophytes in grasses. *The Am. Nat.* **172**, 405–416 (2008).
45. MJ Jeschke, H Kokko, The roles of body size and phylogeny in fast and slow life histories. *Evol. Ecol.* **23**, 867–878 (2009).
46. ME Afkhami, SY Strauss, Native fungal endophytes suppress an exotic dominant and increase plant diversity over small and large spatial scales. *Ecology* **97**, 1159–1169 (2016).

745	47. E Smith, G Vaughan, R Ketchum, D McParland, J Burt, Symbiont community stability	807
746	through severe coral bleaching in a thermally extreme lagoon. <i>Sci. Reports</i> 7 , 2428 (2017).	808
747	48. JW Dallas, RW Warne, Captivity and animal microbiomes: potential roles of microbiota for	809
748	influencing animal conservation. <i>Microb. Ecol.</i> pp. 1–19 (2022).	810
749	49. L Wu, et al., Reduction of microbial diversity in grassland soil is driven by long-term climate	811
750	warming. <i>Nat. Microbiol.</i> 7 , 1054–1062 (2022).	812
751	50. CW Bacon, JF White, Stains, media, and procedures for analyzing endophytes in	813
752	<i>Biotechnology of endophytic fungi of grasses</i> . (CRC Press), pp. 47–56 (2018).	814
753	51. JA Rudgers, AL Swafford, Benefits of a fungal endophyte in <i>elymus virginicus</i> decline under	815
754	drought stress. <i>Basic Appl. Ecol.</i> 10 , 43–51 (2009).	816
755	52. TL Bultman, JF White Jr, TI Bowdish, AM Welch, J Johnston, Mutualistic transfer of	817
756	epichloë spermatia by phorbia flies. <i>Mycologia</i> 87 , 182–189 (1995).	818
757	53. J Gabry, D Simpson, A Vehtari, M Betancourt, A Gelman, Visualization in bayesian	819
758	workflow. <i>J. Royal Stat. Soc. Ser. A: Stat. Soc.</i> 182 , 389–402 (2019).	820
759	54. SP Brooks, A Gelman, General methods for monitoring convergence of iterative simulations.	821
760	<i>J. computational graphical statistics</i> 7 , 434–455 (1998).	822
761	55. A Gelman, J Hill, <i>Data analysis using regression and multilevel/hierarchical models</i> .	823
762	(Cambridge university press), (2006).	824
763	56. JL Williams, TE Miller, SP Ellner, Avoiding unintentional eviction from integral projection	825
764	models. <i>Ecology</i> 93 , 2008–2014 (2012).	826
765	57. OR Jones, et al., Rcompadre and rage—two r packages to facilitate the use of the	827
766	compadre and comadore databases and calculation of life-history traits from matrix	828
767	population models. <i>Methods Ecol. Evol.</i> 13 , 770–781 (2022).	829
768	58. (year?).	830
769	59. PC Bürkner, brms: An R package for Bayesian multilevel models using Stan. <i>J. Stat. Softw.</i>	831
770	80 , 1–28 (2017).	832
771	60. AE Zanne, et al., Three keys to the radiation of angiosperms into freezing environments.	833
772	<i>Nature</i> 506 , 89–92 (2014).	834
773	61. A Leuchtmann, CW Bacon, CL Schardl, JF White Jr, M Tadych, Nomenclatural realignment	835
774	of neotyphodium species with genus epichloë. <i>Mycologia</i> 106 , 202–215 (2014).	836
775	62. CJE Metcalf, et al., Statistical modelling of annual variation for inference on stochastic	837
776	population dynamics using integral projection models. <i>Methods Ecol. Evol.</i> 6 , 1007–1017	838
777	(2015).	839
778	63. H Caswell, Matrix population models: Construction, analysis, and interpretation. 2nd edn	840
779	sinauer associates. Inc., Sunderland, MA (2001).	841
780	64. M Rees, SP Ellner, Integral projection models for populations in temporally varying	842
781	environments. <i>Ecol. Monogr.</i> 79 , 575–594 (2009).	843
782		844
783		845
784		846
785		847
786		848
787		849
788		850
789		851
790		852
791		853
792		854
793		855
794		856
795		857
796		858
797		859
798		860
799		861
800		862
801		863
802		864
803		865
804		866
805		867
806		868

Figures

869	931
870	932
871	933
872	934
873	935
874	936
875	937
876	938
877	939
878	940
879	941
880	942
881	943
882	944
883	945
884	946
885	947
886	948
887	949
888	950
889	951
890	952
891	953
892	954
893	955
894	956
895	957
896	958
897	959
898	960
899	961
900	962
901	963
902	964
903	965
904	966
905	967
906	968
907	969
908	970
909	971
910	972
911	973
912	974
913	975
914	976
915	977
916	978
917	979
918	980
919	981
920	982
921	983
922	984
923	985
924	986
925	987
926	988
927	989
928	990
929	991
930	992

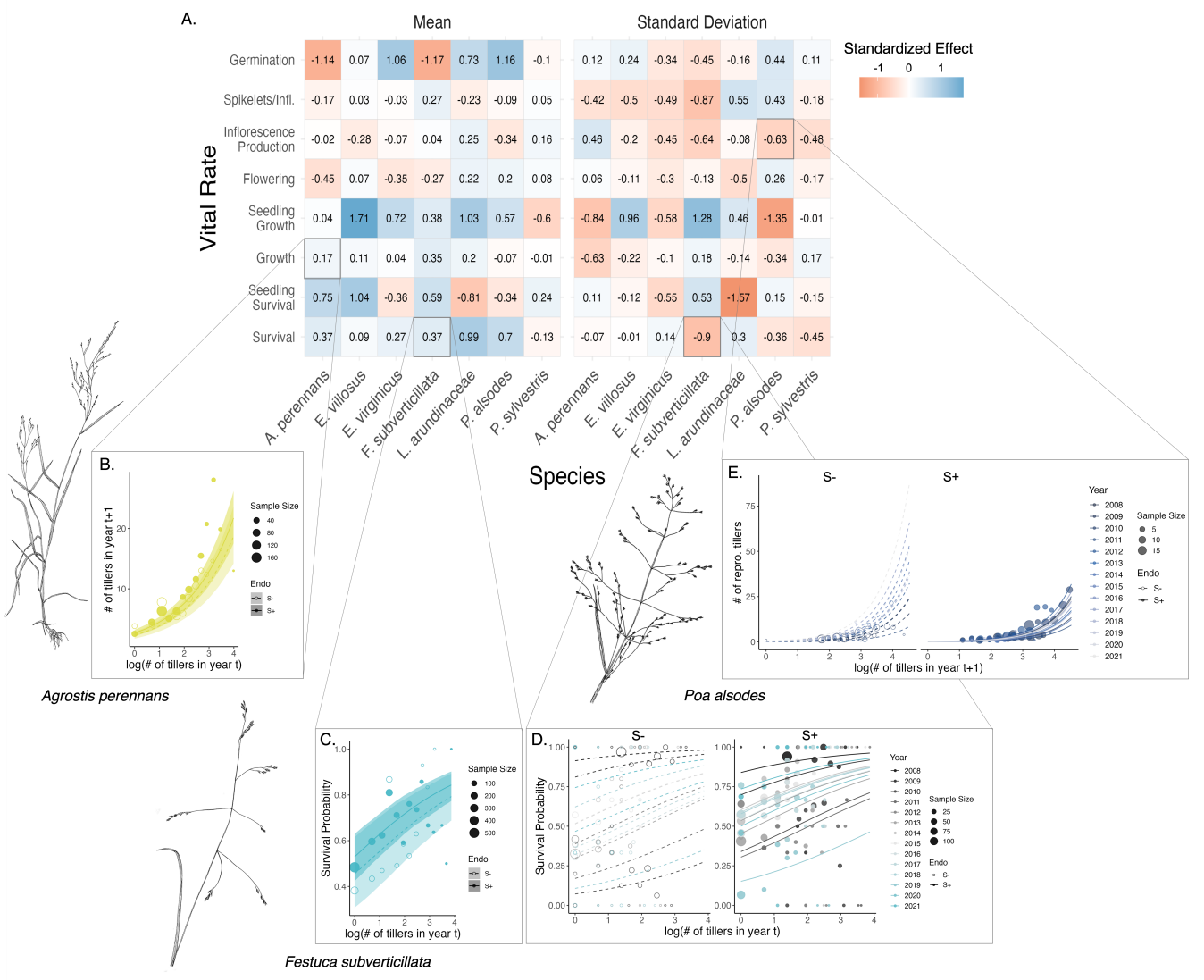


Fig. 1. Endophyte symbiosis altered host vital rates.(A) Shading represents the posterior mean standardized effect size (Cohen's D) of endophyte symbiosis on mean or standard deviation of host vital rates (blue indicates that symbiosis increased the mean or standard deviation and red indicates a reduction). Endophytes' diverse vital rate effects include increased (B) mean growth of *A. perennans* and (C) mean survival probability of *F. subverticillata*. Endophyte presence also reduced inter-annual variance in (D) the survival of *F. subverticillata* and (E) the fertility of *P. alsodes*. Organism silhouettes modified from "Festuca subverticillata" by Cindy Roché and "Agrostis hyemalis" and "Poa alsodes" by Sandy Long ©Utah State University.

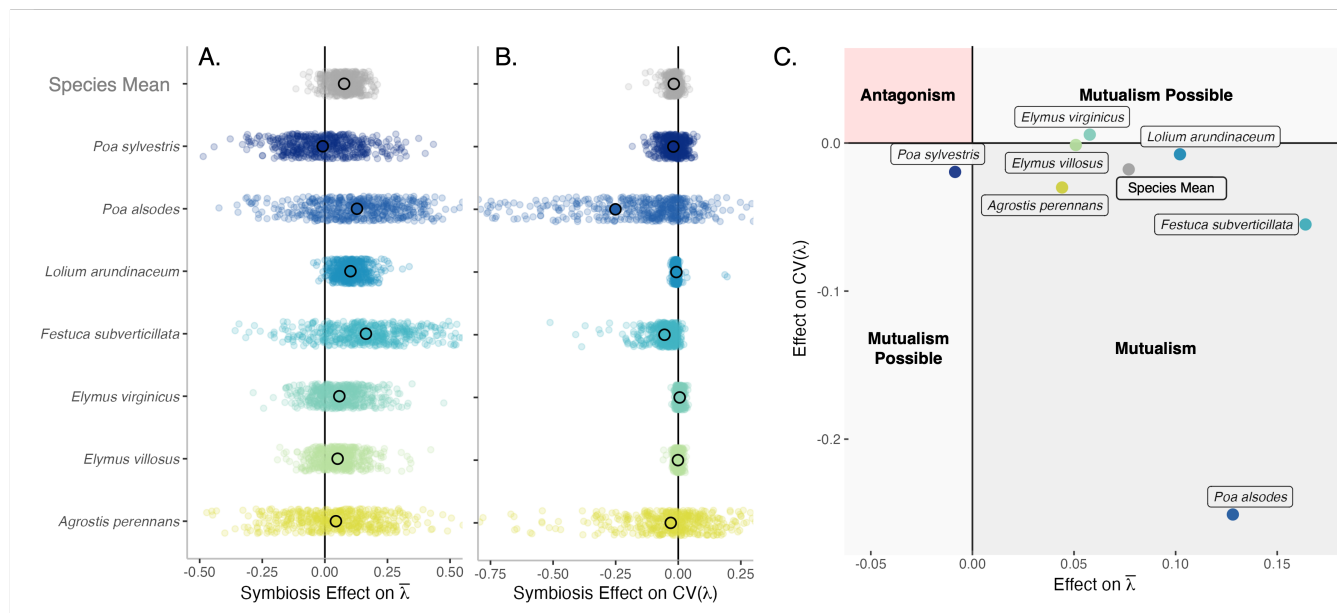


Fig. 2. Mean and variance-buffering effects on fitness. Black circles indicate the average effect of endophytes along with 500 posterior draws (smaller colored circles) on the (A) mean and (B) coefficient of variation in λ for each host species as well as a cross species mean. (C) For all hosts, endophytes either reduce variance, increase the mean, or both, and consequently when considering stochastic environments, the interactions are always at least potentially mutualistic.

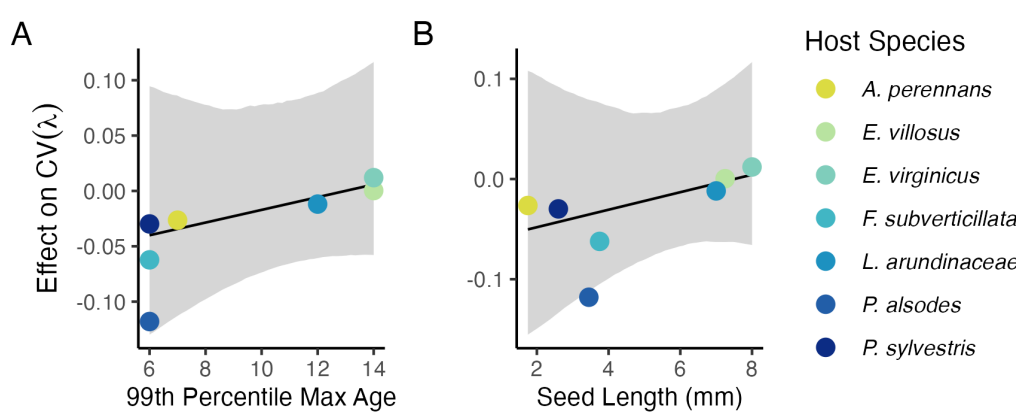


Fig. 3. Host species with faster life history traits experience stronger effects of symbiont-mediated variance buffering. Regressions between life history traits describing the fast-slow life history continuum ((A) 99th percentile maximum age observed during long term censuses in years; (B) Seed size) and the effect of endophyte symbiosis on the coefficient of variation in population growth rate (λ). Each panel shows the fitted mean relationship (line) along with the 95% credible interval.

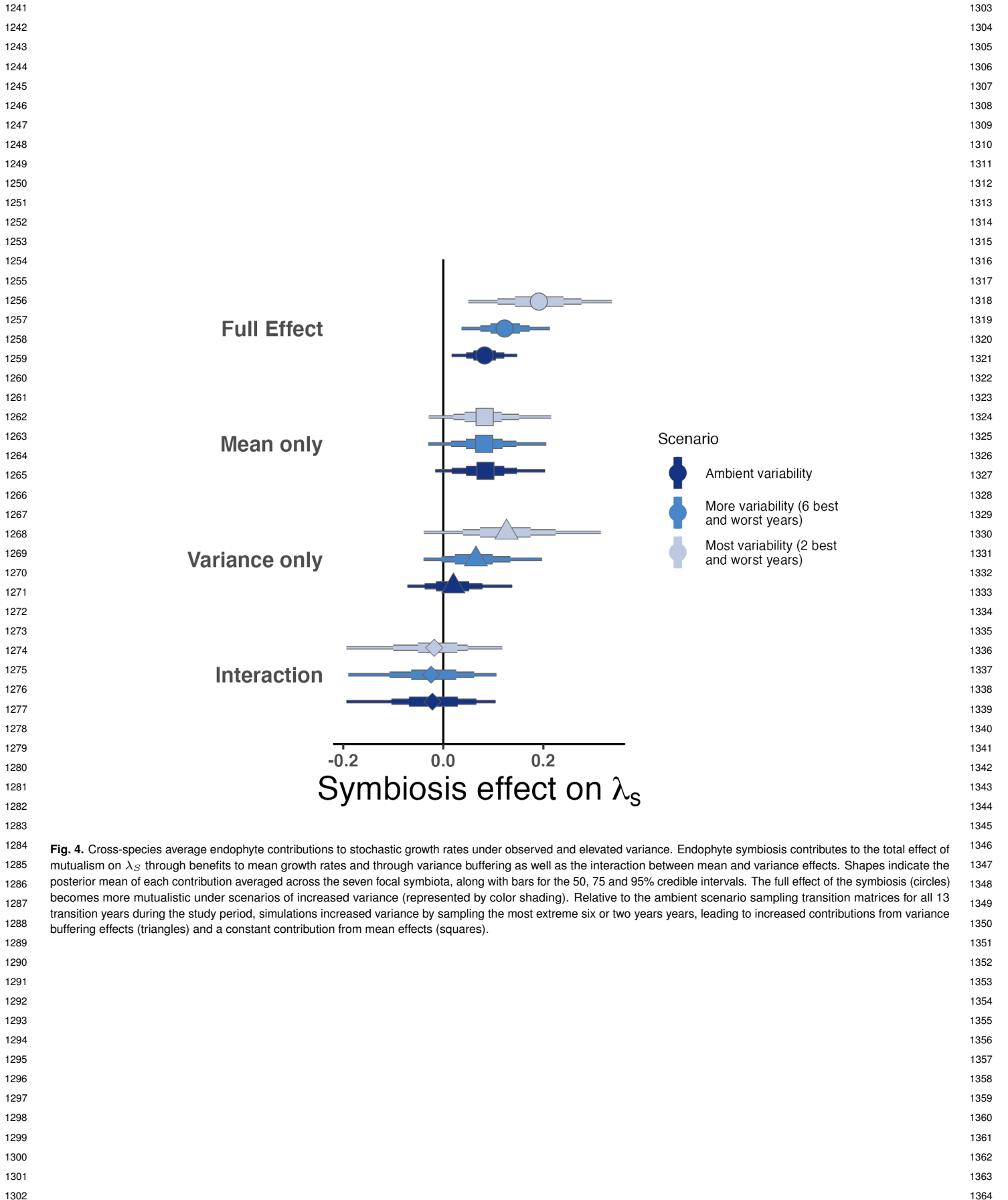


Fig. 4. Cross-species average endophyte contributions to stochastic growth rates under observed and elevated variance. Endophyte symbiosis contributes to the total effect of mutualism on λ_S through benefits to mean growth rates and through variance buffering as well as the interaction between mean and variance effects. Shapes indicate the posterior mean of each contribution averaged across the seven focal symbionts, along with bars for the 50, 75 and 95% credible intervals. The full effect of the symbiosis (circles) becomes more mutualistic under scenarios of increased variance (represented by color shading). Relative to the ambient scenario sampling transition matrices for all 13 transition years during the study period, simulations increased variance by sampling the most extreme six or two years years, leading to increased contributions from variance buffering effects (triangles) and a constant contribution from mean effects (squares).